Biosensors and Bioelectronics 33 (2012) 75–81

Contents lists available at SciVerse ScienceDirect

Biosensors and Bioelectronics

journal homepage: www.elsevier.com/locate/bios

Fabrication and application of amperometric glucose biosensor based on a novel PtPd bimetallic nanoparticle decorated multi-walled carbon nanotube catalyst

Kuan-Jung Chen [a], Chia-Feng Lee [a], John Rick [a], Shih-Han Wang [b], Chung-Chiun Liu [c], Bing-Joe Hwang [a,*]

[a] Nanoelectrochemistry Laboratory, Department of Chemical Engineering, National Taiwan University of Science and Technology, Taipei 106, Taiwan, ROC
[b] Department of Chemical Engineering, I-Shou University, Kaohsiung County 84001, Taiwan, ROC
[c] Department of Chemical Engineering and Electronics Design Center, Case Western Reserve University, 10900 Euclid Avenue, OH44106, USA

ARTICLE INFO

Article history:
Received 12 October 2011
Received in revised form 5 December 2011
Accepted 14 December 2011
Available online 23 December 2011

Keywords:
Pt-based bimetallic nanoparticles (NPs)
PtPd NPs-decorated multi walled carbon nanotube catalyst
Glucose amperometric sensor
Hydrogen peroxide sensing

ABSTRACT

A sensitive, selective and stable amperometric glucose biosensor employing novel PtPd bimetallic nanoparticles decorated on multi-walled carbon nanotubes (PtPd-MWCNTs) was investigated. PtPd-MWCNTs were prepared by a modified Watanabe method, and characterized by XRD and TEM. The biosensor was constructed by immobilizing the PtPd-MWCNTs catalysts in a Nafion film on a glassy carbon electrode. An inner Nafion film coating was used to eliminate common interferents such as uric acid, ascorbic acid and fructose. Finally, a highly porous surface with an orderly three-dimensional network enzyme layer (CS-GA-GOx) was fabricated by electrodeposition. The resulting biosensor exhibited a good response to glucose with a wide linear range (0.062–14.07 mM) and a low detection limit 0.031 mM. The biosensor also showed a short response time (within 5 s), and a high sensitivity (112 $\mu A\,mM^{-1}\,cm^{-2}$). The Michaelis–Menten constant (K_m) was determined as 3.3 mM. In addition, the biosensor exhibited high reproducibility, good storage stability and satisfactory anti-interference ability. The applicability of the biosensor to actual serum sample analysis was also evaluated.

© 2011 Elsevier B.V. All rights reserved.

1. Introduction

A biosensor contains a bioreceptor (such as an enzyme) and a suitable transducer, this combination can be chosen to have unique advantages in terms of: specificity, low-cost, portability, and a fast response time (Malhotra and Chaubey, 2003). A large group of biosensors are based on various oxidases, e.g. glucose oxidase and cholesterol oxidase. From the specific oxidase mediated reaction, hydrogen peroxide (H_2O_2) is produced (1).

$$\text{Analyte} + O_2 \xrightarrow{\text{Oxides}} \text{Byproduct} + H_2O_2 \quad (1)$$

The H_2O_2 can be detected by chemiluminescence (Hanaoka et al., 2001), spectral techniques (He et al., 2006), and electrochemical methods (Hrapovic et al., 2004). Among these, the electrochemical methods are preferred because of their specificity, user-friendliness, high sensitivity, fast response time, and the general need for only low-cost equipment.

Electrochemical biosensors based upon nanomaterials have recently attracted considerable attention. Some examples are Ir, Rh, Pt, Pd, Ag nanoparticles (NPs) assembled on different forms of carbon supports, e.g. E-TEK carbon, graphite, carbon nanofiber, and carbon nanotubes. The fascinating physical and chemical properties of carbon nanotubes such as their electrical conductance, high mechanical stiffness, light weight, electron-spin resonance, field emission, electrochemical actuation, transistor behavior, piezoresistance, contact resistance, coulomb drag power generation, thermal conductivity, luminescence, electrochemical bond expansion, opto-mechanical actuation, and the possibility of introducing functionalization to change their intrinsic properties are reasons for the increasing interest in their use in novel biosensors (Iijima, 1991; Wang, 2004; Merkoci, 2006; Gong et al., 2005; Veetil and Ye, 2007). Pt-based metal NPs-based hybrid nanocomposites have been found to exhibit good catalytic activity towards the redox reduction of H_2O_2 (Wang et al., 1993, 1994, 1996; Ming et al., 2006; Huang et al., 2008; Guo and Dong, 2009; Zhang et al., 2011). Bimetallic nanoparticle-assemblies are of recent origin and are of particular importance in catalysis, since the addition of the second metal brings about variations in particle size, shape, surface morphology, chemical and physical properties including catalytic activity and chemical selectivity. With the advent of new synthetic routes, surface analyzing techniques and surface science modeling facilities, it has become possible to design and prepare tailor-made bimetallic NPs with desired properties. Specifically, Pt-based bimetallic systems with NPs of different structures (alloyed NPs, mixed monometallic NPs, core-shell NPs) have proved

* Corresponding author. Fax: +886 2 27376644.
E-mail address: bjh@mail.ntust.edu.tw (B.-J. Hwang).

0956-5663/$ – see front matter © 2011 Elsevier B.V. All rights reserved.
doi:10.1016/j.bios.2011.12.020

themselves as novel architectures with remarkably improved catalytic and electrocatalytic activity; thus, they are now used extensively for both methanol oxidation and the oxygen reduction reaction in fuel cells (Lim et al., 2009; Chang et al., 2010; Kim et al., 2010; Tao et al., 2008; Stamenkovic et al., 2007).

Immobilization of an enzyme onto a substrate (matrix) is a crucial step in the construction of an enzyme based biosensor. Chitosan (CS) is a biocompatible polymer and has remained a focus of study as one of the most promising materials for enzyme immobilization, due to its hydrophilicity, remarkable biocompatibility and low cost (Kaushik et al., 2008; Li et al., 2008a,b; Li et al., 2006). In addition, CS is a pH shift polymer because it possesses amino groups with a p*K*a of about 6.3. Consequently, the solubility and the net charge of CS are pH-dependent. CS has many primary amino groups, and a p*K*a value of ~6.3. At pH values sufficiently below the p*K*a, CS exists as a water-soluble cationic polyelectrolyte, since most of the amino groups are protonated. When the solution pH is raised to near or above the p*K*a, many of the amino groups are deprotonated, and CS becomes insoluble. Usually, electrochemical deposition of CS is performed via water reduction to yield a hydrogel that can be tightly attached to the electrode, thereby allowing it to retain its natural properties (Wu et al., 2002, 2003, 2005; Xi et al., 2008; Luo et al., 2004). At reducing potentials, H^+ in the solution is consumed at the cathode. Using the locally generated H^+ gradient, the acidic side chains of CS can be titrated, thereby changing the solubility of CS, leading to the controlled deposition of a CS film.

Here the bimetallic nanoparticles decorated on multi-walled carbon nanotubes (PtPd-MWCNTs) catalyst was prepared by a modified Watanabe process employing microwave heating. Transmission electron microscopy (TEM) and X-ray diffraction (XRD) results show the presence of Pt-based bimetallic nanoparticles PtPd with mean diameters of 3.2 nm. The catalyst layer was fabricated by drop coating method. The resulting PtPd-MWCNTs nanocomposite film offers new capabilities for electrochemical devices resulting from the synergistic action of PtPd bimetallic nanaoparticles and MWCNTs. The anti-interference layer (Nafion) was coated on the PtPd-MWCNT nanocomposite film surface. The biosensor was fabricated by immobilizing the CS-GA-glucose oxidase (GOx) enzyme layer onto the electrode's surface by electrodeposition. The electrochemical behavior of the modified electrode was been investigated by cyclic voltammetry (CV), electrochemical impedance spectroscopy (EIS) and amperometry. The resulting biosensor exhibits high sensitivity, good reproducibility, long-term stability with notable freedom from interference from co-existing electroactive species.

2. Experimental

2.1. Apparatus and reagents

$H_2PtCl_6{\cdot}3H_2O$ and Na_2PdCl_4 were purchased from ACROS. GOx, EC 1.1.3.4; Type X-S from *Aspergillus niger*, 155,000 unit g^{-1},) and CS from shrimp shells (≥75% deacetylated) were purchased from Sigma–Aldrich. The platinum nanoparticles dispersed carbon (20 wt.% Pt) and palladium nanoparticles dispersed carbon (20 wt.%) was purchased from E-TEK, Inc. (Taiwan), and BASF, Inc. (Taiwan), respectively. The MWCNTs (95% purity, 20–40 nm diameter) were purchased from Scientech Co. (Taiwan). Prior to use, the MWCNTs were purified by refluxing in HNO_3–H_2SO_4 (v/v, 1:1) at 90 °C for 8 h, filtered, washed thoroughly with deionized (DI) water and dried at room temperature. The supporting electrolyte was phosphate buffer solution (PBS) containing 0.1 M Na_2HPO_4–NaH_2PO_4 + 0.10 M KCl (pH 7.4), all other chemicals were of analytical grade and used without further purification. Solutions were prepared and diluted using ultra-pure water (Millipore Milli Q system). Electrochemical experiments were performed with an Autolab PGSTAT302N electrochemical analyzer (AUTOLAB, USA) with a conventional three electrode cell. The working electrode was a glassy carbon electrode (GCE, diameter 5 mm). A saturated calomel electrode (SCE) and a platinum wire electrode were used as the reference and counter electrodes, respectively. Electrochemical measurements of the modified GCE and bare GCE were performed in 0.1 M PBS (containing $Fe(CN)_6^{3-}$ and $Fe(CN)_6^{4-}$ (both 10 mM) + 0.1 M KCl, pH 7.4) by CV and EIS. The frequency range was between 0.1 and 100,000 Hz with signal amplitude of 10 mV. XRD patterns for the final PtPd-MWCNTs sample were obtained on a diffractometer (Rigaku Dmax-B, Japan) using a Cu Kα source operating at 40 kV and 100 mA with a scan rate of 0.05 deg^{-1} for 2θ values between 20° and 90°. TEM examination was performed on a Philips Tecnai F20G2 FEI-TEM microscope operating with an accelerating voltage of 200 keV. The EDX measurements were performed with a JSM 6500 EDX analyzer. Specimens were prepared by ultrasonically suspending the catalyst powders in ethanol, applying the specimen to a copper grid and drying in air. Scanning electron microscopy (SEM) image were obtained at 5.0 keV on a Hitachi S-240 JOEL JSM-6500F field emission SEM.

2.2. Synthesis of bimetallic PtPd NPs-coated MWCNTs catalysts (PtPd-MWCNTs)

The PtPd-MWCNTs were prepared using the colloidal reduction method developed by Watanabe et al. with a slight modification (Watanabe et al., 1987; Hwang et al., 2006). Here, the pH of the aqueous $H_2PtCl_6{\cdot}3H_2O$ (3.47 mM) and Na_2PdCl_4 (3.05 mM) solutions were adjusted to 7 and 4, respectively, with 1 M Na_2CO_3 followed by reduction by $NaHSO_3$ to their corresponding intermediate compounds. To each of the precursor solutions H_2O_2 was added and the pH was maintained at 6 using 1 M NaOH. The two solutions were mixed and the pH maintained at 7. An appropriate amount of MWCNTs (to maintain 20 wt.% of total metal in the composite) were added, and the mixture heated at 100 °C for 4 h. The resulting colloidal product was washed with ultra-pure water and dried. Hydrogen reduction was performed on the colloidal product by passing a gas mixture comprising 10% H_2 + 90% Ar through the material in a furnace kept at 250 °C for 1 h to form the bimetallic NPs-coated MWCNTs. The metal loading (Pt + Pd) was maintained at 20 wt.% in order to allow comparison with the commercial catalysts ETK-20 Pt–C and BASF Pd–C. For the Pt-MWCNTs and Pd-MWCNTs catalyst preparations, aqueous $H_2PtCl_6{\cdot}3H_2O$ (5.13 mM) and Na_2PdCl_4 (9.40 mM) solutions were used respectively.

2.3. Fabrication of Nafion/PtPd-MWCNTs/GCE

A 0.5 wt.% Nafion stock solution was prepared by diluting the 5 wt.% Nafion with ethanol. Catalyst (6 mg) was dispersed in dimethylformamide (3 mL) containing 1.5 mL of Nafion (0.5 wt.%) and sonicated for 1 h. Prior to surface modification, the glassy carbon electrodes were polished with alumina powder (0.3, and 0.05 μm) to obtain a mirror finish. The electrodes were then sonicated for 5 min, thoroughly rinsed with ethanol and DI water, and dried under a nitrogen stream. A 15 μL aliquot of catalyst solution was drop cast on the GCE surface and allowed to dry at room temperature to form the PtPd-MWCNTs/GCE. Finally, Nafion solution (5 μL, 0.2 wt.%) was cast on the surface of the prepared electrode. The prepared electrodes (Nafion/PtPd-MWCNTs/GCE) were stored in a refrigerator (4 °C), when not in use.

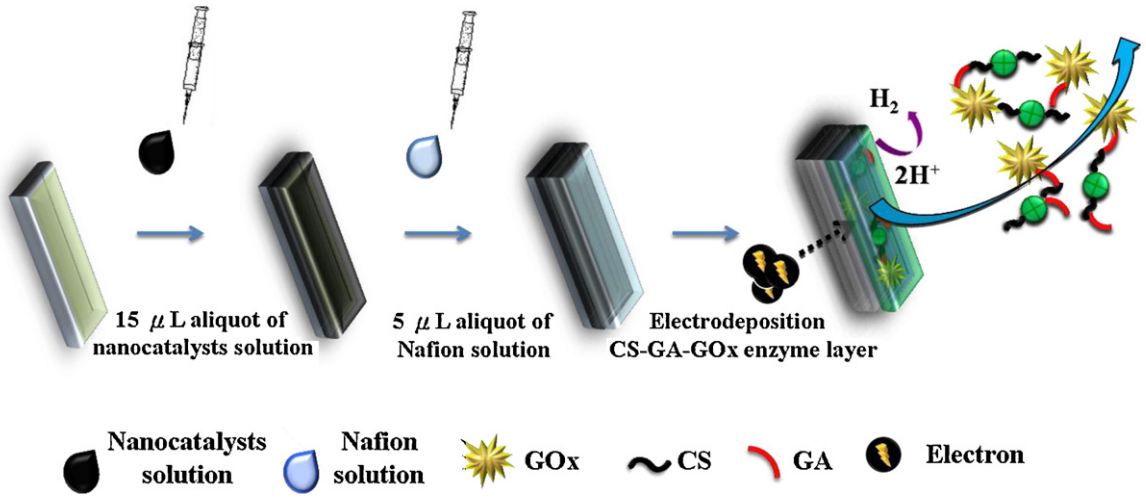

Scheme 1. The fabricating procedure for the CS-GA-GOx/Nafion/PtPd-MWCNTs/GCE.

2.4. Fabrication of enzyme electrode CS-GA-GOx/Nafion/PtPd-MWCNTs/GCE

A homogenous mixture containing CS, and GOx was prepared as the electrodeposition solution for fabrication of the enzyme layers. CS aqueous solution (0.2 wt.%) was prepared according to a previously reported procedure (Li et al., 2009). Briefly, CS solid was dissolved in aqueous HCl (0.01 M) and the pH adjusted to 5.0 using 0.5 M NaOH, any undissolved particles were filtered using a 0.45 μm cellulose film. GOx (25.0 mg) was added to 5.0 mL of a CS solution [0.20 wt.% (pH 5.0)] with magnetic stirring, GA aqueous solution (4 μL, 25 wt.%) was added slowly with vigorous magnetic stirring, followed by 4 h reaction at 4 °C for pre-crosslinking (Tana et al., 2010). For the electrodeposition, Nafion/PtPd-MWCNTs/GCE

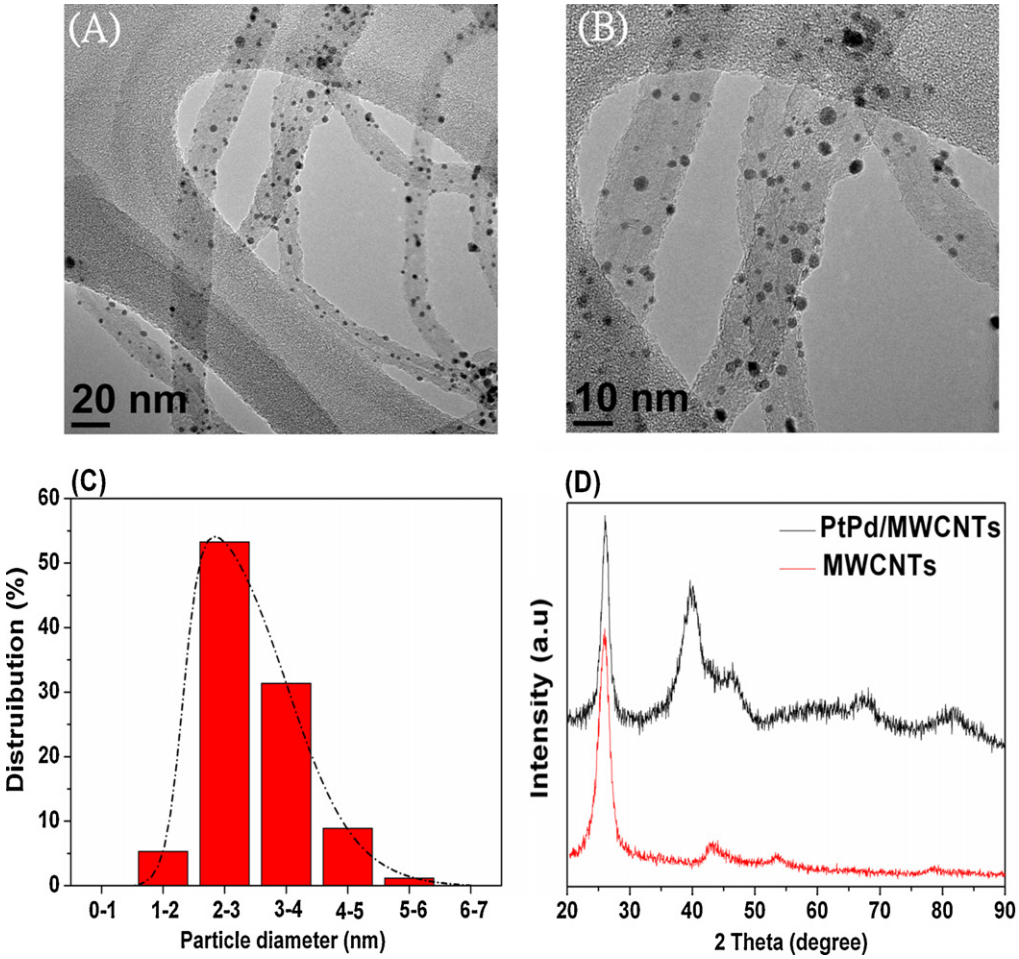

Fig. 1. TEM images of catalysts: 20 wt.% PtPd-MWCNTs (A) low magnification, (B) high magnification, and (C) corresponding histograms of size distribution, (D) XRD patterns of MWCNTs and catalyst 20 wt.% PtPd-MWCNTs.

was immersed in the above solution and used as the cathode by applying a constant current density (410 μA cm^{-2}) for 120 s. In the electrodeposition, GOx was entrapped in situ in the CS gel and the enzyme layer was formed. The obtained electrode (CS-GA-GOx/Nafion/PtPd-MWCNTs/GCE) was washed with 0.1 M PBS and dried at room temperature for about 15 min, and then stored at 4 °C in the dry state for 12 h before use. The biosensor fabrication processes is shown in Scheme 1.

3. Results and discussion

3.1. Characterization of catalysts

Fig. 1(D) shows the XRD patterns of PtPd-MWCNTs. The peaks located at 26.2° in all the XRD patterns can be assigned to the (0 0 2) hexagonal structure of the MWCNTs. The other four peaks are characteristic of face centered cubic (FCC) crystalline Pt (JCPDS-ICDD, Card No. 04-802), corresponding to the planes (1 1 1), (2 0 0), (2 2 0), and (3 1 1) at 2θ of ca. 40°, 48°, 70° and 84°, respectively. The average grain sizes of the catalysts were calculated by the Scherrer's equation (Radmilovic et al., 1995). From the results, it was found that the average grain size of PtPd-MWCNTs was around 3.1 nm. The atomic compositions and the total metal loadings of the fabricated PtPd-MWCNTs catalysts were determined by EDX and ICP. The results reveal that the Pt to Pd atomic ratio (0.702:0.298) and the total metal loading (19.4 wt.%) are close to their nominal values for PtPd-MWCNTs catalysts prepared by the modified Watanabe method. The TEM images show that the nano-sized particles to be spherical and highly dispersed on the MWCNTs with no particle aggregation being observed (Fig. 1(A)). The size distribution was evaluated statistically by measuring the diameter of 200 PtPd nanoparticles in selected TEM images. The PtPd particle sizes are distributed mainly between 1.6 and 5.5 nm (average diameter 3.2 nm, see Fig. 1(C)). The high-resolution TEM (HRTEM) image shows that the graphitic sheets and bimetallic nanoparticles (PtPd) of the PtPd-MWCNTs had a highly ordered crystalline structure as shown in Fig. 1(B).

3.2. Characterization of modified GCE

The electrochemical performances of the bare GCE, PtPd-MWCNTs/GCE, Nafion/PtPd-MWCNTs/GCE, and CS-GA-GOx/Nafion/PtPd-MWCNTs/GCE electrodes were investigated using CV with $Fe(CN)_6^{3-/4-}$ as a redox probe. As shown in Fig. 2(A), the redox peak shapes at the bare GCE were rather broad and the peak potential separation (ΔE_p, $\Delta E_p = E_{pa} - E_{pc}$) was as large as 235 mV (curve a). In contrast, with GCE modified with PtPd/MWCNTs, the peak separation decreased significantly and both the ferricyanide anodic and cathodic peak currents (I_p) increased quite considerably, suggesting improved electron transfer and mass transfer, both facilitated by the huge surface area provided by the extended three dimensional structure of the PtPd-MWCNTs (curve b). After the Nafion film had been immobilized on the electrode's surface, the peak current decreased and the peak separation increased (curve c), suggesting the negatively charged (sulfonated) Nafion severely reduced the effective area and therefore the number of active sites available for electron transfer. After the CS-GA-GOx biocomposite film had been electrodeposited on the Nafion/PtPd-MWCNTs/GCE surface, the peak currents of the system reduced to a minimum, while the peak separation reached a maximum. This may be due to the bulky CS and GOx molecules blocking electron exchange between the redox probe and electrode's surface (curve d).

As controls the CVs and electrochemical characterization of Pt-MWCNTs/GCE, Pd-MWCNTs/GCE and MWCNTs/GCE were recorded and measured. The results showed the marked superiority in performance of the MWCNTs bearing Pt/Pd. The data from these investigations are shown in Supplementary information S1.

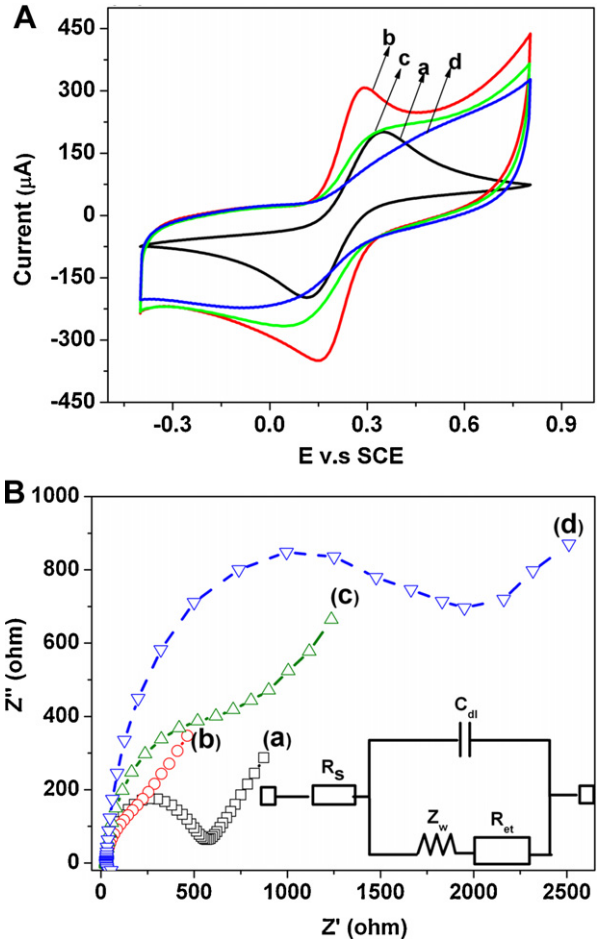

Fig. 2. (A) Cyclic voltammograms of the electrode modified with different components scan rate, 50 mV s^{-1}. (a) Bare GCE, (b) PtPd-MWCNTs/GCE, (c) Nafion/PtPd-MWCNTs/GCE, (d) CS-GA-GOx/Nafion/PtPd-MWCNTs/GCE, (B) EIS of the different electrodes: (a) Bare GCE, (b) PtPd-MWCNTs/GCE, (c) Nafion/PtPd-MWCNTs/GCE, (d) CS-GA-GOx/Nafion/PtPd-MWCNTs/GCE, Supporting electrolyte, 10 mM $Fe(CN)_6^{3-/4-}$ + 0.1 M KCl + 0.1 M (pH 7.4) PBS. The frequency range is between 0.1 and 100,000 Hz (AC 10 mV, DC 0.25 V versus SCE).

EIS is an effective technique for probing the features of surface modified electrodes. The impedance spectra include a semicircle portion and a linear portion. Fig. 2(B) shows the EIS of the electrode at different stages. The EIS of the bare GCE displays a small semicircle at high frequencies, corresponding to the electron-transfer resistance (R_{et}), and a linear region, corresponding to the diffusion process, at low frequencies (curve a), suggesting a very low R_{et} (528 Ω) to redox probe $Fe(CN)_6^{3-/4-}$. For the bare GCE modified with PtPd-MWCNTs, it can be seen that (curve b) is almost a straight line with a very low R_{et} on PtPd-MWCNTs/GCE, implying that the catalysts had excellent electrical conductivity and thereby accelerated electron transfer. Subsequently, when the Nafion film was coated on the surface of PtPd-MWCNTs/GCE, the R_{et} for the redox probe increased to (983 Ω) (curve c), suggesting the negatively charged (sulfonated) Nafion film had a reduced effective area for electron transfer. However, R_{et} increased to (2003 Ω) after electrodeposition of CS-GA-GOx biocomposite film (curve d), suggesting that the enzyme layer formed an additional barrier and isolated the redox probe from the electrode's surface. To analyze the electrode's impedance characteristics a modified Randles equivalent circuit (inset Fig. 2(B)) was chosen to fit the measured results. The two components of the scheme, R_s and Z_w, represent the bulk

properties of electrolyte solution and diffusion of the applied redox probe, respectively. The C_{dl} depends on the dielectric at the electrode/electrolyte interface. These results are consistent with the CV tests.

The surface morphologies of PtPd-MWCNTs/GCE, Nafion/PtPd-MWCNTs/GCE and CS-GA-GOx/Nafion/PtPd-MWCNTs/GCE were studied by SEM as shown in (Supplementary information Figs. S1(A)–(C)). PtPd-MWCNTs/GCE showed a uniform surface topography, while the PtPd-MWCNT film was a three dimensional network like structure (shown in Supplementary information Fig. S1(A)). This porous structure is potentially able to increase the electrode's effective surface area and thus facilitate the diffusion of analytes into the nanocomposite film. For comparison, SEM images of the Nafion film on the PtPd-MWCNTs/GCE surface, showed a relatively smooth surface (Supplementary information Fig. S1(A)). Supplementary information Fig. S1(C) represents the SEM image of the CS-GA-GOx biocomposite film. It was found that the biocomposite film formed by electrodeposition possessed a highly porous surface. As a result, GOx was incorporated in situ into the three dimensional network of the biocompatible CS gel. Such a morphological structure might improve the probe's diffusion characteristics and thus contribute to the good sensitivity and fast response of the biosensor.

3.3. Electrochemical performance of the Nafion/PtPd-MWCNTs/GCE towards the H_2O_2 sensing

Fig. 3(A) shows the typical amperometric response of the Nafion/PtPd/MWCNTs/GCE for successive additions of H_2O_2 at an applied potential of 0.6 V. As shown in the inset (a), the time to achieve 95% steady state current for the Nafion/PtPd-MWCNTs/GCE was no more than 5 s. The fast response may be due to the facile diffusion of H_2O_2 in the nanocomposite film. As shown in Fig. 3(B), the calibration is linear over a wide concentration range (0.012–14 mM): the linear regression equation is $I\ (\mu A\,cm^{-2}) = 393\ (\mu A\,cm^{-2})C\ (mM) + 116\ (\mu A\,cm^{-2})$ with a coefficient of determination (R^2) = 0.993. The sensitivity and the detection limit were 393 $\mu A\,mM^{-1}\,cm^{-2}$ and 0.008 mM respectively; the insert (b) in Fig. 3(A) shows the signal-to-noise ratio to be ~3. Repeated use of the electrode did not degrade performance or reproducibility due to the stability of the assembled film. For example, 2 mM H_2O_2 was measured continuously 10 times, and a relative standard deviation (R.S.D.) of 2.9% was obtained. The excellent electrocatalytic activity of the electrode suggests it may be used as a new electrochemical platform for incorporating a large number of oxidase-based enzymes.

3.4. Amperometric determination of glucose at the enzyme electrode

Fig. 4(A) shows a typical current–time plot for the enzyme electrode (CS-GA-GOx/Nafion/PtPd-MWCNTs/GCE) upon successive additions of 0.031 mM, and 1.2 mM glucose at 0.6 V. The current response of the enzyme electrode increased with increasing glucose concentration. As shown in the inset (a), the CS-GA-GOx biocomposite film modified electrode reached 95% of the steady-state current within 5 s. The fast response can be attributed to two factors: first, the PtPd-MWCNTs nanocomposite film not only provides a high surface area and excellent electrical conductivity, but also improves electrocatalytic activity, thus allowing rapid electro-oxidation of the H_2O_2; second, the CS matrix has a thin and highly porous structure, thereby facilitating fast substrate diffusion. Fig. 4(A) inset (b) shows the calibration curve of glucose at the enzyme electrode as a linear response to glucose from 0.062 mM to 14.07 mM (R^2 = 0.997), the linear regression equation is $I\ (\mu A\,cm^{-2}) = 112\ (\mu A\,cm^{-2})C\ (mM) + 134\ (\mu A\,cm^{-2})$. Normal

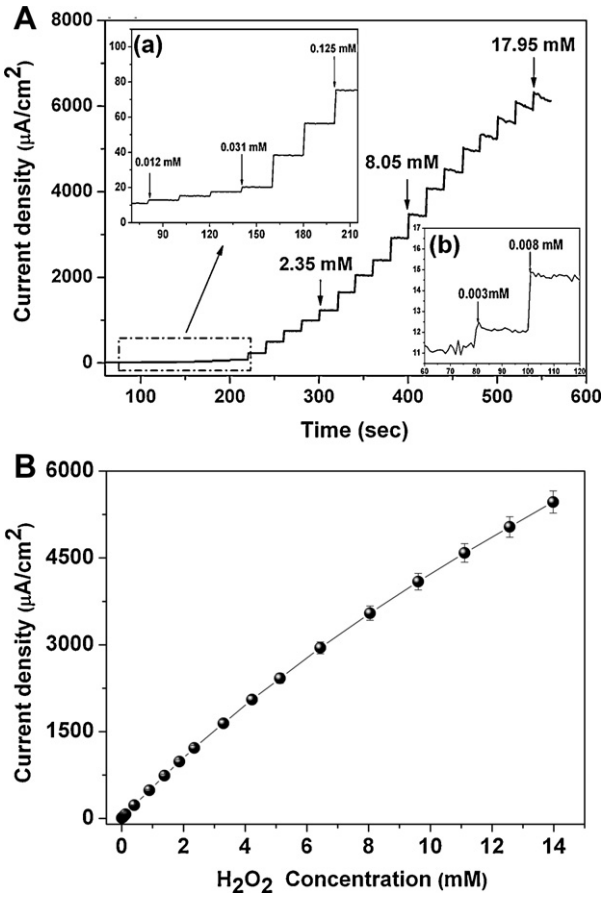

Fig. 3. (A) Current versus time curve of the Nafion/PtPd-MWCNTs/GCE for successive additions of H_2O_2, Inset (a) indicated by arrows with marked concentrations to 0.1 M (pH 7.4) PBS at 0.60 V versus SCE. Inset (b) the detection limit of Nafion/PtPd-MWCNTs/GCE for successive addition 0.003, and 0.008 mM of H_2O_2 (S/N = 3), (B) calibration curve for H_2O_2.

blood glucose levels range from 4 to 6 mM. So the linear glucose response from 0.062 to 14.07 mM makes the enzyme electrode suitable for practical applications in determining blood sugar concentrations. The electrode has a sensitivity of 112 $\mu A\,mM^{-1}\,cm^{-2}$ and a detection limit 0.031 mM with a signal-to-noise ratio of 3. This study also compared with the other two commercial catalysts such as ETK-20 Pt–C and BASF Pd–C used to prepare enzyme electrodes under the same conditions. The performance of these electrodes is shown in Supplementary information Fig. S3. The CS-GA-GOx/Nafion/ETK-20 Pt-C/GCE, showed linearity between 0.062 and 12.8 mM (R^2 = 0.994) with a sensitivity of 97 $\mu A\,mM^{-1}\,cm^{-2}$, while the CS-GA-GOx/Nafion/BASF Pd–C/GCE, showed linearity between 0.062 and 5.99 mM (R^2 = 0.992) with a sensitivity of 47 $\mu A\,mM^{-1}\,cm^{-2}$, thus the higher sensitivity and wide linear range of the enzyme electrode can be attributed to the excellent electrocatalytic activity of the PtPd-MWCNTs catalysts. A comparative study was made of the amperometric sensing of H_2O_2 using a catalyst modified GCE method to evaluate the catalytic behavior of the PtPd-MWCNTs/GCE, ETK-20 Pt-C/GCE and the BASF Pd–C/GCE with similar metal loadings. The PtPd-MWCNTs/GCE exhibited a higher sensitivity (296 $\mu A\,mM^{-1}\,cm^{-2}$) compared to the ETK-20 Pt-C/GCE (271 $\mu A\,mM^{-1}\,cm^{-2}$) and the BASF Pd–C/GCE (17 $\mu A\,mM^{-1}\,cm^{-2}$) at the same applied potential (0.25 V versus SCE) – all measurements taken within the same linear detection range (25–300 μM). The results are given in (Supplementary information Fig. S4). This study also compared the electrode assembly with another two in-house fabricated catalysts i.e. Pt-MWCNTs, Pd-MWCNTs and with bare MWCNTs used to prepare

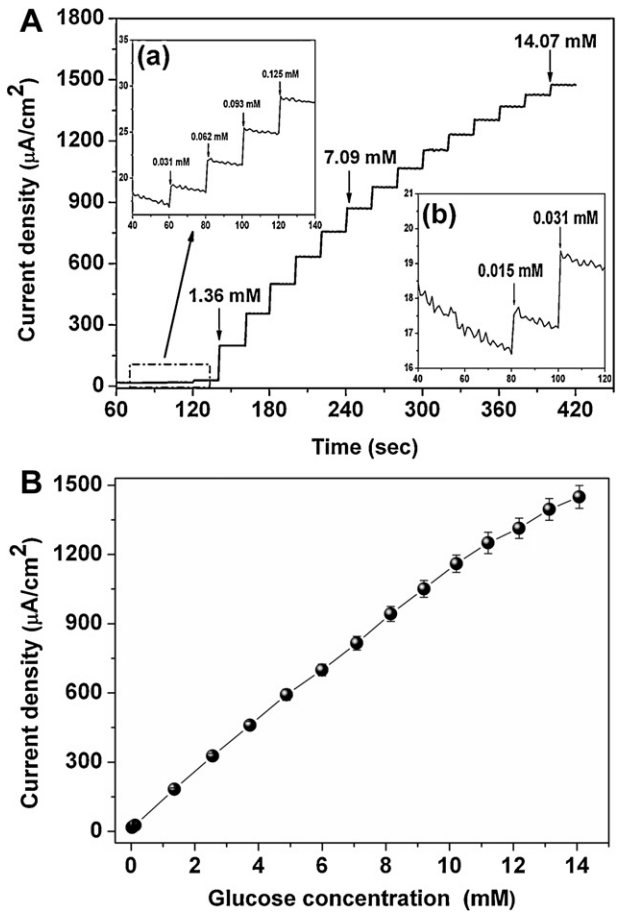

Fig. 4. (A) Current versus time curve of the CS-GA-GOx/Nafion/PtPd-MWCNTs/GCE for successive additions of glucose, Inset (a) indicated by arrows with marked concentrations to 0.1 M (pH 7.4) PBS at 0.60 V versus SCE. Inset (b) the detection limit of CS-GA-GOx/Nafion/PtPd-MWCNTs/GCE for successive addition 0.015, and 0.031 mM of glucose (S/N = 3), (B) calibration curve for glucose.

enzyme electrodes under the same conditions. Data from electrode assemblies with in-house fabricated catalysts are shown in Supplementary information Fig. S5. The CS-GA-GOx/Nafion/Pt-MWCNTs/GCE, curve (a) showed linearity between 0.062 and 8.15 mM ($R^2 = 0.996$) with a sensitivity of 103 μA mM^{-1} cm^{-2}, CS-GA-GOx/Nafion/Pd-MWCNTs/GCE, curve (b) showed linearity between 0.062 and 8.15 mM ($R^2 = 0.993$) with a sensitivity of 51 μA mM^{-1} cm^{-2}, and the CS-GA-GOx/Nafion/MWCNTs/GCE, curve (c) showed linearity between 0.062 and 8.15 mM ($R^2 = 0.947$) with a sensitivity of 6.7 μA mM^{-1} cm^{-2}.

When glucose concentration was high, a plateau current was observed, showing the characteristics of Michaelis–Menten kinetics. The apparent Michaelis–Menten constant (K_m) and the maximum current density (i_{max}) can be obtained by an amperometric method as suggested by Shu and Wilson (1976):

$$\frac{1}{i_s} = \frac{K_m}{i_{max}}\left(\frac{1}{C_g}\right) + \frac{1}{i_{max}}$$

where i_s is the steady-state current, C_g the concentration of glucose, K_m the apparent Michaelis–Menten constant and i_{max} is the maximum current density. From the curve of the i_s^{-1} versus C_g^{-1}, based on the experimental data from Fig. 4(B), the apparent Michaelis–Menten constant K_m and the maximum current density i_{max} were estimated to be 3.3 mM, and 1446.5 μA cm^{-2}, respectively. These results show that the biosensor possesses a high affinity with respect to glucose in solution. The immobilization process might give rise to changes in the microenvironment of the enzyme that affect its intrinsic properties leading to an enhanced affinity for glucose. To support this contention, analytical parameters obtained with different Pt NPs-based amperometric glucose sensors are listed in Table 1, including applied potential, linear range, sensitivity, detection limit, response time and the Michaelis–Menten constant.

3.5. Reproducibility and stability of the enzyme electrode

Reproducibility and long-term stability are important requirements for a reusable sensor. Reproducibility with respect to the enzyme electrode's construction was estimated from the response to 5 mM glucose at five enzyme electrodes prepared under the same conditions. The results revealed that the biosensor has satisfactory reproducibility with a (R.S.D.) of 3.7% as shown in Supplementary information Fig. S6. For long-term stability evaluation, measurements were taken at intervals of one week – the biosensor (when not in use) was stored in a dry condition at 4 °C. After 7 days, the biosensor retained 95% of its original current generating ability, falling to approximately 85% after 28 days.

3.6. Interference tests

Anti-interference properties are also important considerations for sensors. Because easily oxidized species such as ascorbic acid, uric acid and other carbohydrate compounds, (such as fructose) usually co-exist with glucose in human blood, the electrochemical response of the interfering species was also examined, as shown in (Supplementary information Fig. S7). The interference experiment was carried out by successive injections: 0.5 mM interfering species, followed by 0.5 mM glucose, and finally 1 mM glucose into the supporting electrolyte. The result shows that the response signals of AA, UA, and fructose are negligible when present with glucose in an equimolar concentration (0.5 mM). This anti-interference ability is thought to result from the inclusion of the Nafion film

Table 1
Comparison of the performances of the various types of glucose biosensors.

Electrode	Applied potential (V)	Linear range (mM)	Sensitivity (μA mM^{-1} cm^{-2})	LOD (μM)	Response time (s)	K_m (mM)	Reference
GOx/GNPs[a]/MWCNTs/Pt	0.35 (Ag/AgCl)	0.1–10	36.1	6.7	7	14.9	Wu et al. (2007)
GOx-CS-SiO_2/Pt/MWCNT/GCE	0.6 (Ag/AgCl)	0.001–23	58.9	1	5	14.4	Zou et al. (2008)
CS-GA-GOx/PtNPs/Au	0.7 (SCE)	0.001–5.3	102	0.1	–	10.6	Tana et al. (2010)
GOx/GNPs/PtNPs/CNT/Au	0.6 (SCE)	0.5–16.5	–	400	5	11.89	Chu et al. (2007)
GOx-PS[b]-MWNTs/GCE	−0.55 (Ag/AgCl)	0–8	32	0.35	–	–	Gao et al. (2010)
GOD/PtNPs/PIL[c]-CNTs/GCE	0.6 (SCE)	Up to 12	28.28	10	–	–	Chu et al. (2010)
CS-GA-GOx/Nafion/PtPd-MWCNTs/GCE	0.6 (SCE)	0.062–14	112	31	5	3.3	This work

[a] Gold nanoparticles.
[b] Phenosafranine.
[c] Polymerized ionic liquid (1-vinyl-3-ethylimidazolium tetrafluoroborate ([VEIM]BF_4).

that effectively inhibits the penetration of negatively charged substrates (Mao et al., 2000; Shankaran et al., 2003); thus, the presence of these species did not influence glucose determination.

3.7. Application of the enzyme electrode to the determination of glucose in serum

In order to demonstrate practical usage of the biosensor, serum samples were assayed. The serum samples and their glucose concentrations were provided by a local medical examination center. The serum samples were first analyzed with a YSI 2300 STAT Plus Glucose Analyzer. The samples were then re-assayed with the (CS-GA-GOx/Nafion/PtPd-MWCNTs/GCE). Serum samples (3 ml) were added into 2 ml of 0.1 M PBS (pH 7.4), and the response was obtained at 0.6 V. The glucose concentration in the serum was then calculated from the calibration curve Fig. 4(B). The analytical results provided by the YSI glucose analyzer and those determined using the biosensor are listed in Supplementary information Table S2. The close agreement of the two sets of results suggests that the biosensor can be used for serum glucose determinations.

4. Conclusions

In the present work, a novel route for fabricating a biosensor was developed. The bimetallic nanoparticles, having a narrow particle size distribution, were well dispersed on the surface of the multi-walled carbon nanotubes by using a modified Watanabe method. The immobilization of a CS-GA-GOx biocomposite film onto the Nafion/PtPd-MWCNTs/GCE surface was carried out by electrodeposition. The resulting biosensor exhibited a wide linear range from 0.062 mM to 14 mM with a high sensitivity ($112\,\mu A\,mM^{-1}\,cm^{-2}$). The enzyme electrode also demonstrated excellent stability and resistance to interference. The excellent overall performance is attributed to the PtPd-MWCNTs catalytic activity towards H_2O_2 electrooxidation in combination with the good biocompatibility of the chitosan gel. The hybrid nanocomposites provide a new electrochemical platform for designing a variety of bioelectrochemical devices with high sensitivity and good stability.

Acknowledgement

The authors gratefully acknowledge the support from the National Science Council (NSC-97-2120-M-011-001 and NSC-97-2221-E-011-075-MY3), the National Synchrotron Radiation Research Center (NSRRC), the National Taiwan University of Science and Technology and Electronics Design Center of Case Western Reserve University.

Appendix A. Supplementary data

Supplementary data associated with this article can be found, in the online version, at doi:10.1016/j.bios.2011.12.020.

References

Chang, S.H., Su, W.N., Yeh, M.H.C., Pan, J., Yu, K.L., Liu, D.G., Lee, J.F., Hwang, B.J., 2010. Chem. Eur. J. 16, 11064–11071.
Chu, X., Duan, D., Shen, G., Yu, R., 2007. Talanta 71, 2040–2047.
Chu, X., Wu, B., Xiao, C., Zhang, X., Chen, J., 2010. Electrochim. Acta 55, 2848–2852.
Gao, F., Yin, J., Yao, Z., Li, M., Wang, L., 2010. J. Electrochem. Soc. 157 (3), F35–F39.
Gong, K.P., Yan, Y.M., Zhang, M.N., Su, L., Xiong, S.X., Mao, L.Q., 2005. Anal. Sci. 21, 1383–1392.
Guo, S.J., Dong, S.J., 2009. Trends Anal. Chem. 28, 96–109.
Hanaoka, S., Lin, J., Yamada, M., 2001. Anal. Chim. Acta 426, 57–64.
He, F., Tang, Y., Yu, M., Wang, Y., Li, Y., Zhu, D., 2006. Adv. Funct. Mater. 16, 91–94.
Hrapovic, S., Liu, Y., Male, B.K., Luong, J.H.T., 2004. Anal. Chem. 76, 1083–1088.
Huang, J.S., Wang, D.W., Hou, H.Q., You, T.Y., 2008. Adv. Funct. Mater. 18, 441–448.
Hwang, B.J., Chen, C.H., Sarma, L.S., Chen, J.M., Wang, G.R., Tang, M.T., Liu, D.G., Lee, J.F., 2006. J. Phys. Chem. B 110, 6475–6482.
Iijima, S., 1991. Nature 354, 56–58.
Kaushik, A., Khan, R., Solanki, P.R., Pandey, P., Alam, J., Ahmad, S., Malhotra, B.D., 2008. Biosens. Bioelectron. 24, 676–683.
Kim, Y., Hong, J.W., Lee, Y.W., Kim, M., Kim, D., Yun, W.S., Han, S.W., 2010. Angew. Chem. 49, 10197–10201.
Li, F., Chen, W., Tang, C.F., Zhang, S.S., 2008a. Talanta 77, 1–8.
Li, F., Li, J., Zhang, S.S., 2008b. Talanta 74, 1247–1255.
Li, F., Wang, Z., Chen, W., Zhan, S., 2009. Biosens. Bioelectron. 24, 3030–3035.
Li, F., Li, X.M., Zhang, S.S., 2006. J. Chromatogr. A 1129, 223–230.
Lim, B., Jiang, M., Camargo, P.H.C., Cho, E.C., Tao, J., Lu, X., Zhu, Y., Xia, Y., 2009. Science 324, 1302–1305.
Luo, X.L., Xu, J.J., Du, Y., Chen, H.Y., 2004. Anal. Biochem. 334, 284–289.
Malhotra, B.D., Chaubey, A., 2003. Sens. Actuators B-Chem. 91, 117–127.
Mao, L., Yamaomoto, K., Zhou, W., Jin, L., 2000. Electroanalysis 12 (1), 72–77.
Merkoci, A., 2006. Microchim. Acta 152, 157–174.
Ming, L., Xi, X., Liu, J., 2006. Biotechnol. Lett. 28, 1341–1345.
Radmilovic, V., Gasteiger, H.A., Ross, P.N., 1995. J. Catal. 15, 98–106.
Shankaran, D.R., Uehara, N., Kato, T., 2003. Biosens. Bioelectron. 18 (5–6), 721–728.
Shu, F.R., Wilson, G.S., 1976. Anal. Chem. 48, 1679–1686.
Stamenkovic, V.R., Mun, B.S., Arenz, M., Mayrhofer, K.J.J., Lucas C.A., Wang, G., Ross, P.N., Markovic, N.M., 2007. Nat. Mater. 6, 241–247.
Tana, Y., Denga, W., Chena, C., Xiea, Q., Lei, L., Li, Y., Fanga, Z., Maa, M., Chen, J., Yaoa, S., 2010. Biosens. Bioelectron. 25, 2644–2650.
Tao, F., Grass, M.E., Zhang, Y., Butcher, D.R., Renzas, J.R., Liu, Z., Chung, J.Y., Mun, B.S., Salmeron, M., Somorjai, G.A., 2008. Science 322, 932–934.
Veetil, J.V., Ye, K.M., 2007. Biotechnol. Prog. 23, 517–531.
Wang, J., 2004. Electroanalysis 17, 7–14.
Wang, J., Fang, L., Lopez, D., Tobias, H., 1993. Anal. Lett. 2, 1819–1830.
Wang, J., Liu, J., Chen, L., Lu, F., 1994. Anal. Chem. 66, 3600–3603.
Wang, J., Rivas, G., Chicharro, M., 1996. Electroanalysis 8, 434–451.
Watanabe, M., Uchida, M., Motoo, S., 1987. J. Electroanal. Chem. 229, 395–406.
Wu, L.Q., Gadre, A.P., Yi, H., Kastantin, M.J., Rubloff, G.W., Bentley, W.E., Payne, G.F., Ghodssi, R., 2002. Langmuir 18, 8620–8625.
Wu, L.Q., Lee, K., Wang, X., English, D.S., Losert, W., Payne, G.F., 2005. Langmuir 21, 3641–3646.
Wu, L.Q., Yi, H., Li, S., Rubloff, G.W., Bentley, W.E., Ghodssi, R., Payne, G.F., 2003. Langmuir 19, 519–524.
Wu, B.Y., Hou, S.H., Yin, F., Zhao, Z.X., Wang, Y.Y., Wang, X.S., Chen, Q., 2007. Biosens. Bioelectron. 22, 2854–2860.
Xi, F.N., Liu, L.J., Wu, Q., Lin, X.F., 2008. Biosens. Bioelectron 24, 29–34.
Zhang, Y., Sun, Y., Liu, Z., Xu, F., Cui, K., Shi, Y., Wen, Z., Li, Z., 2011. J. Electroanal. Chem. 656, 23–28.
Zou, Y., Xiang, C., Sun, L.X., Xu, F., 2008. Biosens. Bioelectron. 23, 1010–1016.